

NASA/TP- 20210025470



Adaptation To Environmental Extremes Structures Functional Traits in Biological Soil Crust and Hypolithic Microbial Communities

*Rachel Mackelprang
California State University Northridge, Biology Department*

*Parag Vaishampayan
NASA Ames Research Center*

*Kirsten Fisher
California State University, Los Angeles, Department of Biological Sciences*

December 2021

NASA STI Program Report Series

The NASA STI Program collects, organizes, provides for archiving, and disseminates NASA's STI. The NASA STI program provides access to the NTRS Registered and its public interface, the NASA Technical Reports Server, thus providing one of the largest collections of aeronautical and space science STI in the world. Results are published in both non-NASA channels and by NASA in the NASA STI Report Series, which includes the following report types:

- **TECHNICAL PUBLICATION.** Reports of completed research or a major significant phase of research that present the results of NASA Programs and include extensive data or theoretical analysis. Includes compilations of significant scientific and technical data and information deemed to be of continuing reference value. NASA counterpart of peer-reviewed formal professional papers but has less stringent limitations on manuscript length and extent of graphic presentations.
- **TECHNICAL MEMORANDUM.** Scientific and technical findings that are preliminary or of specialized interest, e.g., quick release reports, working papers, and bibliographies that contain minimal annotation. Does not contain extensive analysis.
- **CONTRACTOR REPORT.** Scientific and technical findings by NASA-sponsored contractors and grantees.
- **CONFERENCE PUBLICATION.** Collected papers from scientific and technical conferences, symposia, seminars, or other meetings sponsored or co-sponsored by NASA.
- **SPECIAL PUBLICATION.** Scientific, technical, or historical information from NASA programs, projects, and missions, often concerned with subjects having substantial public interest.
- **TECHNICAL TRANSLATION.** English-language translations of foreign scientific and technical material pertinent to NASA's mission.

Specialized services also include organizing and publishing research results, distributing specialized research announcements and feeds, providing information desk and personal search support, and enabling data exchange services.

For more information about the NASA STI program, see the following:

- Access the NASA STI program home page at <http://www.sti.nasa.gov>
- E-mail your question to help@sti.nasa.gov
- Phone the NASA STI Information Desk at 757-864-9658

NASA/TP- 20210025470



Adaptation To Environmental Extremes Structures Functional Traits in Biological Soil Crust and Hypolithic Microbial Communities

*Rachel Mackelprang
California State University Northridge, Biology Department*

*Parag Vaishampayan
NASA Ames Research Center*

*Kirsten Fisher
California State University, Los Angeles, Department of Biological Sciences*

National Aeronautics and
Space Administration

Ames Research Center

December 2021

1 **Title:**

2 Adaptation to environmental extremes structures functional traits in biological soil crust and
3 hypolithic microbial communities

4 **Authors:**

5 Rachel Mackelprang¹, Parag Vaishampayan², Kirsten Fisher³

6 **Affiliations:**

7 1. California State University Northridge, Biology Department. 18111 Nordhoff St.
8 Northridge, CA, 91130. rachel.mackelprang@gmail.com

9
10 2. Space Biosciences Division, NASA Ames Research Center, Moffett Field, CA 94035,
11 USA. Parag.a.vaishampayan@nasa.gov

12
13 3. California State University, Los Angeles, Department of Biological Sciences. 5151
14 State University Dr. Los Angeles, CA, 90032. kfisher2@exchange.calstatela.edu

15 **Corresponding authors:**

16 Rachel Mackelprang and Kirsten Fisher

17 **Keywords:**

18 Biological soil crusts, environmental microbiology, metagenomics, moss, cyanobacteria, desert
19 ecosystems, extreme environments

20
21
22

23 Abstract

24 Biological soil crusts (biocrusts) are widespread in drylands and deserts. At the microhabitat
25 scale, they also host hypolithic communities that live under semi-translucent stones. Both
26 environmental niches experience exposure to extreme conditions such as high UV radiation,
27 desiccation, temperature fluctuations, and resource limitation. However, hypolithic communities
28 are somewhat protected from extremes relative to biocrust communities. Conditions are
29 otherwise similar, so comparing them can answer outstanding questions regarding adaptations to
30 environmental extremes. Using metagenomic sequencing, we assessed the functional potential of
31 dryland soil communities and identified the functional underpinnings of ecological niche
32 differentiation in biocrusts versus hypoliths. We also determined the effect of the anchoring
33 photoautotroph (moss or cyanobacteria). Genes and pathways differing in abundance between
34 biocrusts and hypoliths indicate that biocrust communities adapt to the higher levels of UV
35 radiation, desiccation, and temperature extremes through an increased ability to repair damaged
36 DNA, sense and respond to environmental stimuli, and interact with other community members
37 and the environment. Intracellular competition appears to be crucial to both communities, with
38 biocrust communities waging war using the Type VI Secretion System (T6SS) and hypoliths
39 favoring diversity of antibiotics. The dominant primary producer had a reduced effect on
40 community functional potential compared with niche, but an abundance of genes related to
41 monosaccharide, amino acid, and osmoprotectant uptake in moss-dominated communities
42 indicates reliance on resources provided to heterotrophs by mosses. Our findings indicate that
43 functional traits in dryland communities are driven by adaptations to extremes and we identify
44 strategies that likely enable survival in dryland ecosystems.

45

46 **Importance**

47 Biocrusts serve as a keystone element of desert and dryland ecosystems, stabilizing soils,
48 retaining moisture, and serving as a carbon and nitrogen source in oligotrophic environments.
49 Biocrusts cover approximately 12% of the Earth’s terrestrial surface but are threatened by
50 climate change and an anthropogenic disturbance. Given their keystone role in ecosystem
51 functioning, loss will have wide-spread consequences. Biocrust microbial constituents must
52 withstand polyextreme environmental conditions including high UV exposure, desiccation,
53 oligotrophic conditions, and temperature fluctuations over short time scales. By comparing
54 biocrust communities with co-occurring hypolithic communities (which inhabit the ventral sides
55 of semi-translucent stones and are buffered from environmental extremes), we identified traits
56 that are likely key adaptations to extreme conditions. These include DNA damage repair,
57 environmental sensing and response, and intracellular competition. Comparison of the two
58 niches, which differ primarily in exposure levels to extreme conditions, makes this system ideal
59 for understanding how functional traits are structured by the environment.

60

61 **Introduction**

62 Biological soil crusts (biocrusts) are communities anchored by primary producers such as
63 cyanobacteria, mosses, algae, and lichens, and accompanied by diverse bacteria, archaea, and
64 fungi (1). In deserts and drylands, biocrusts occupy the first few millimeters of the soil surface,
65 where they perform multiple functions, including nutrient capture and erosion control (2, 3).
66 Globally, biocrusts cover approximately 12% of the Earth’s terrestrial surface (4) and contribute
67 significantly to soil stability, hydrology, and carbon and nitrogen cycling at ecosystem scales (1).
68 At the microhabitat scale, drylands sometimes support hypolithic niches on the ventral side of
69 semi-translucent stones (usually quartz) embedded in the soil surface (5). Hypoliths can occur in
70 hyper extreme habitats too harsh to support exposed biocrusts (6–9), but they are also found as
71 dispersed microsites within areas supporting more extensive biocrusts (10).

72 Biocrust organisms are physiologically specialized for survival in polyextreme
73 environments characterized by challenges such as high (and low) temperatures, desiccation,
74 intense UV radiation, and nutrient limitation (11). To survive in these conditions, organisms in
75 the community are typically poikilohydric, capable of equilibrating to the ambient relative
76 humidity of their environment and suspending all metabolic activity in a dried and quiescent
77 state. Once water is re-introduced, poikilohydric organisms resume metabolic activity almost
78 instantaneously through a combination of cellular protective mechanisms deployed during drying
79 (e.g., ROS scavenging, compatible solutes, mRNPs) and repair mechanisms initiated upon
80 rehydration (12–15). For larger biocrust organisms (e.g., mosses) that may require extensive
81 cellular repair upon rewetting from the desiccated state, the process of rehydration is
82 energetically costly and creates a carbon deficit that must be recovered through a period of
83 photosynthetic activity (16, 17). Thus, while biocrusts are physiologically specialized for

84 environments with low precipitation, they are sensitive to the frequency, timing, and duration of
85 hydration events (18).

86 In habitats where biocrusts occur, drying events happen quickly relative to the time
87 required for poikilohydric organisms to launch extensive cellular protective processes. Thus,
88 biocrust organisms tend to rely heavily on cellular repair during rehydration as their strategy for
89 tolerating desiccation (19). Although these repair mechanisms are highly efficient (20) larger
90 biocrust organisms such as mosses lose some cellular contents during the process of membrane
91 repair during rehydration, which in turn may provide a nutritional resource to support a diverse
92 community of heterotrophic microbes, a phenomenon coined the ‘bryotic pulse’ (21).

93 Photoautotrophs (cyanobacteria, mosses, and lichens) anchor biocrust communities, both
94 physically (i.e., soil aggregation, hydrological controls) and through primary production.
95 Typically, biocrusts are dominated by one type of photoautotroph, which in turn influences the
96 diversity and abundance of other organisms in the community (10, 22, 23). The identity of the
97 dominant photoautotroph also influences biocrust multifunctionality and community stability in
98 the presence of climate perturbations (24–27).

99 The identity of the dominant photoautotroph and taxonomic composition of the rest of the
100 community is at least partially dictated by predictable successional processes (28, 29). Bare soils
101 are first colonized by filamentous cyanobacteria such as *Microcoleus*, which aggregates soil
102 particles with its polysaccharide sheaths and generates organic carbon to support a diverse
103 community of heterotrophic bacteria, including diazotrophs, within the cyanosphere (30). Later
104 successional stages are characterized by darkly pigmented nitrogen-fixing cyanobacteria like
105 *Scytonema*, followed eventually by mosses and/or lichens (22). While cyanobacteria are typically
106 the major photoautotroph found in hypolithic communities (5, 31), some hypoliths support

107 mosses (5, 10, 32–34). Previous taxonomic work indicated some compositional overlap in
108 microbial communities supported by hypoliths and moss-dominated biocrusts (10), but the extent
109 to which hypolith communities may be functionally distinct from surrounding biocrusts is
110 unknown.

111 Building on previous work demonstrating that biocrust photoautotrophs affect the
112 taxonomic composition of their associated microbial communities (10, 22) and biocrust
113 ecophysiology/multifunctionality (22, 24, 25, 35), we investigated the degree to which niches
114 (biocrust or hypolithic microsites) harbor communities with distinct functional repertoires using
115 a comparative metagenomics approach. We also assessed the effect of dominant photoautotroph
116 (moss, cyanobacteria) on microbial traits to assess the degree to which the photoautotroph anchor
117 might support communities with distinct functional pathways. Specifically, we set out to test the
118 following hypotheses: **(1)** Hypolithic microsites within regions supporting biocrusts should
119 harbor their own distinct microbial communities enriched in pathways reflective of lower levels
120 of heat and desiccation stress relative to surrounding biocrusts. **(2)** The presence of moss in
121 biocrust creates an important nutritional resource due to the ‘leakiness’ of gametophyte tissues,
122 and moss biocrusts should support communities with pathways that reflect the utilization of
123 diverse substrates provided by moss leakage in an oligotrophic environment. We sampled
124 replicate cyanobacteria- and moss-dominated biocrusts and hypoliths from two distinct habitats
125 in the Mojave Desert of California. Metagenomic sequence data generated from these samples
126 were then analyzed to compare functional potential across different biocrust and primary
127 producer types to identify adaptive strategies related to survival in extreme dryland
128 environments.

129

130

131 **Methods**

132 **Field Site and Sample Collection**

133 Soil and biocrust samples were collected on March 25, 2018 from the Sheep Creek Wash
134 near Wrightwood, CA. The Sheep Creek Wash site is located at the northern base of the San
135 Gabriel Mountains (34°22'33.85"N, 117°36'34.59"W) and the western edge of the Mojave Desert
136 at an elevation of 1800 m (36). A second site in the UC Sweeny Granite Mts. Reserve
137 (34°47'08.3"N 115°39'36.2"W, 1280 m elevation), located along the southwestern edge of the
138 Mojave National Preserve, was visited for collection on Aug 3-4, 2018. Both sites were chosen
139 based on the co-occurrence of biocrusts and hypoliths containing the moss *Syntrichia caninervis*
140 as the dominant photosynthetic anchor species within the same restricted (~ 3 m²) area (36). *S.*
141 *caninervis* was identified based on characteristics such as hair points on the apices of leaves, leaf
142 morphology, and colony pigmentation. Seven replicate samples were collected for each of the
143 following microsite types: hypolith with moss; hypolith without moss (cyanobacteria only); moss
144 biocrust; cyanobacterial biocrust; soil ca. 1 cm below each of these microsite types; and non-
145 biocrust surface soil. A sterile spatula (surface sterilized with 70% isopropyl alcohol between
146 samples) was used to collect of 5-10 g soils and biocrusts, and each sample was placed individually
147 into a sterile Nasco Whirl Pak bag (Fort Atkinson, WI). For hypolithic samples, quartz rocks (often
148 with visible adhered microbial biomass) were collected along with soil and associated organisms.
149 All samples were stored on ice during field collection and transported back to the lab, where they
150 were stored at -20 °C until DNA extraction.

151

152

153

154 **DNA Extraction and Sequencing**

155 Quartz samples were crushed with a UV sterilized hammer to obtain biological matter
156 adhered to the rock samples. Smaller rocks were scraped using a sterile scalpel to gather
157 biological materials for DNA extraction. For samples containing moss biocrusts, ca 5 stems of
158 moss were first submerged for several seconds (using sterile forceps) in the buffer used during
159 the cell disruption step of the DNA extraction protocol to remove some of the adhered soil and
160 biocrust material for subsequent DNA extractions. Care was taken to remove all traces of moss
161 after submersion. The prepared samples then underwent DNA extraction using a FastDNA SPIN
162 Kit for Soil (MP Biomedicals, Irvine, CA) according to the manufacturer's instructions (with the
163 addition of the moss-washing step noted above). Quantification readings were taken immediately
164 after DNA extraction using a Qubit 4 fluorometer (Invitrogen, Carlsbad, CA). Libraries were
165 prepared at the Department of Energy Joint Genome Institute and sequenced (2x150) on the
166 Illumina NovaSeq platform (Illumina Inc., San Diego, CA) (Walnut Creek, CA; GOLD Study
167 ID: Gs0136120; GOLD Sequencing Project IDs: Gp0356221 - Gp0356280). Additional
168 accession numbers are found in Supplemental Table 1.

169 **Annotation and Statistical Analyses**

170 Reads derived from *S. caninervis* (37), the dominant moss species, were removed using
171 bbduk.sh (version updated October 10 2020) from the BBtools suite of programs (38).
172 Functional annotation of reads was performed by comparison to the Kyoto Encyclopedia of
173 Genes and Genomes (KEGG) database (39) using DIAMOND (v0.9.30.131) (40) with an E-
174 value cutoff of $1e-6$. Reads were assigned a KEGG Orthology (KO) number according to the top
175 hit. The resulting KO annotation data were summarized in a gene count matrix. We applied a low
176 abundance filter, where genes observed more than 100 times in at least 10% of the samples were

177 retained. Relationships between samples were visualized using Principle Coordinate Analysis
178 based on Bray-Curtis dissimilarities using the phyloseq package (41) in R (42). Alpha diversity
179 (Shannon index) was also calculated using phyloseq. Differences in alpha diversity among
180 samples were evaluated using ANOVA followed by a Tukey post-hoc test. Permutational
181 Multivariate Analysis of Variance (PERMANOVA) was performed using the adonis function in
182 the vegan package in R (43). Genes whose abundances differed between groups were identified
183 using a quasi-likelihood negative binomial generalized linear model implemented in the edgeR
184 package (44). For individual genes, we used a conservative adjusted P-value threshold of $P <$
185 0.01. Heatmaps were generated using the R pheatmap package (45). Rows and columns within
186 the heatmap were clustered using the complete linkage method for the purpose of visualization.

187 We identified differentially abundant pathways using a method we developed previously
188 (46). Briefly, we placed genes onto KEGG pathway maps and counted the number of genes in
189 each pathway that were significantly more abundant in one category versus another (i.e., biocrust
190 versus hypolith, hypolith versus biocrust, moss- versus cyanobacteria-dominated, and
191 cyanobacteria- versus moss-dominated). For each of the sample category comparisons, we then
192 randomly assigned P-values to each gene from the observed set of P-values. 10,000 permutations
193 were performed, generating a null distribution of the number of significantly different genes
194 expected in each pathway. Pathways differing significantly between sample categories were
195 identified by assigning P-values based on how often the number of significant genes in the
196 permutations exceeded the observed number of significant genes in each pathway. The resulting
197 P-values were corrected using the false discovery rate (47). Significant pathways were manually
198 inspected and removed if the majority of significant genes were broadly distributed across many
199 pathways. We implemented this conservative measure so that pathways reaching significance

200 due to a high abundance of “promiscuous” genes rather than actual functional enrichment were
201 not considered in downstream analyses.

202

203 **Results**

204 **Factors driving differences among sites**

205 We performed metagenomic sequencing on 60 samples from biocrusts, hypoliths, and
206 bare soil at an average depth of 9.06 Gb per sample for a total of 534 Gb (Supplemental Table 1).
207 Reads were annotated by comparison to the KEGG gene database (Supplemental Table 2).
208 Ordinations of KEGG gene count data revealed clear differences in genetic repertoire between
209 biocrust and hypolith communities (Figure 2A). When ordinations of biocrust and hypolith
210 communities were plotted separately, samples clustered by the dominant primary producer
211 (cyanobacteria or moss) (Figure 2B-C).

212 To determine the effect of environmental niche (biocrust, hypolith, bare soil), dominant
213 primary producer (cyanobacteria, moss), sampling location/season (Sheep Creek Wash/March
214 versus UC Sweeny Granite Mountains Reserve/August), and sample depth (within the biocrust
215 or hypolith versus below) on microbial functional potential we performed permutational
216 multivariate analysis of variance (PERMANOVA) tests on KEGG gene count data. Functional
217 potential differed significantly between biocrust, hypolith, and bare soil samples ($F=3.58$, $R^2 =$
218 0.09 $P=0.005$) but no other single factor was significant. Environmental niche and primary
219 producer interactions had the strongest effect on microbial community functional potential,
220 explaining 11.4% of the variation in diversity ($F=9.27$, $P = 0.001$). Primary Producer x Layer and

221 Primary Producer x Collection site/month interactions had much smaller (but significant) effects
222 on functional potential (Supplemental Table 3).

223 Alpha diversity differed significantly among sample types (ANOVA, $F=12.76$, $P=7.29e-$
224 10 , Supplemental Figure 1). Diversity was highest in the moss-associated biocrusts and lowest in
225 the samples from below moss-associated biocrusts and hypoliths. Samples where cyanobacteria
226 were the dominant primary producer had similar diversity regardless of environmental niche
227 (biocrust or hypolith) or layer (below or within).

228

229 **Genes and pathways differentiating biocrust and hypolith communities.**

230 Because environmental niche had the strongest effect on gene relative abundances, we
231 first focused our analyses on the genes (Supplemental Tables 4 & 5) and pathways (Tables 1 &
232 2) differing significantly between biocrust and hypolith communities. Those that were more
233 abundant in biocrusts were largely related to survival in extreme environments. Specifically,
234 DNA damage repair, environmental sensing and response via the two-component regulatory
235 system, biofilm formation, motility, and the ability to interact and compete via the bacterial
236 secretion system (Table 1). Pathways significantly more abundant in hypolith communities were
237 dominated by secondary metabolite synthesis, including antibiotic biosynthesis (Table 2).

238

239 **Genes and pathways enriched in biocrust versus hypolith communities**

240 Commensurate with elevated environmental exposure to UV and desiccation, DNA repair
241 gene frequencies were higher biocrusts than in hypoliths. At the level of pathway, this was
242 shown by a significant enrichment of the KEGG homologous recombination pathway ($P=0.018$)

243 and a nearly significant enrichment of the mismatch repair pathway ($P=0.058$). These
244 observations prompted us to investigate specific genes in both these and other DNA repair
245 pathways that were more abundant in biocrust versus hypolith samples. We identified twenty-
246 two significant DNA repair genes ($P<0.01$) with a wide range of repair functions, including
247 double strand break, single strand break, mismatch, base and nucleotide excision repair, and
248 replication restart (Figure 3, Supplemental Table 6). Six subunits of DNA polymerase III, which
249 is involved in the repair processes listed above and in DNA replication, were also significantly
250 enriched in biocrusts.

251 The two-component regulatory system is the major means bacteria use to sense
252 environmental signals and modify behavior or physiology accordingly (48). We found that the
253 KEGG two-component system pathway was significantly more abundant in biocrusts compared
254 with hypoliths ($P < 0.001$, Table 1). Significant genes ($P < 0.01$) within the pathway were
255 grouped into three primary categories: lifestyle, redox signals and catabolites, and nutrient
256 limitation and stress (Figure 4, Supplemental Table 7). Within the lifestyle category, all genes for
257 the chemosensory pathway of bacterial chemotaxis, the Wsp chemosensory pathway for biofilm
258 formation, and the CckA-ChpT-CtrA phosphorelay system (potentially controlling motility and
259 biofilm formation (49, 50)) were significant. Multiple genes from other chemosensory systems
260 related to twitching motility, quorum sensing, and biofilm formation were also significant
261 (Figure 4A). In the redox signals and catabolites category (Figure 4B), we found that both genes
262 in the conserved RegB/RegA signal transduction system, which controls a large number of
263 energy-generating and energy-using processes (51), were significant. Other significant genes in
264 this category include those for sensing oxidation states, anaerobic respiration, catabolite
265 repression, and C4-Dicarboxylate transport. Finally, significant genes within the nutrient

266 limitation and stress category indicate that biocrust community members are better able to sense
267 and respond to low nutrient availability (particularly iron, phosphate, Mg^{2+} , and nitrogen) and
268 certain stressors (osmotic stress, acidic conditions, and oxygen limitation) (Figure 4C). We also
269 note that RNA polymerase sigma-54 factor, which plays a role in stress response (52) and
270 interacts with multiple two component systems, was significantly more abundant in biocrusts
271 than in hypolith communities.

272 Providing additional evidence for an increased capacity for motility, the KEGG bacterial
273 flagellar assembly pathway was significantly more abundant in biocrust versus hypolith
274 communities ($P < 0.01$, Table 1). Thirty-six of 54 (66.7%) genes within the pathway were
275 significant ($P < 0.01$, Figure 5, Supplemental Table 8). When genes with a narrow phylogenetic
276 distribution were excluded (H and T ring genes), 75% were significant. The KEGG chemotaxis
277 pathway was also enriched in biocrusts ($P < 0.01$), which was expected because it includes many
278 of the same two-component system genes described previously (Supplemental Table 9). In the
279 biofilm formation pathway (Supplemental Table 10), significant genes included Type IV pilus
280 formation and the Type II secretion system.

281 Bacterial secretion systems are sophisticated protein complexes that transport proteins,
282 small molecules, and DNA into the extracellular milieu or into target cells. The bacterial
283 secretion system KEGG pathway, which includes six secretion systems (types I through IV) and
284 two accessory transport systems (sec and tat), was significantly more abundant in biocrusts than
285 in hypoliths ($P < 0.001$). To determine which of the systems were enriched in biocrust
286 communities, we identified the genes encoding secretion system components that were likewise
287 significant (Figure 6, Supplementary Table 11). We found that four of the six secretion systems
288 (types I, II, IV, and VI) and the sec accessory system were enriched in biocrusts. Eight of the

289 nine genes forming the Type VI secretion system (T6SS), which is one of the main weapons of
290 interbacterial competition, were significantly more abundant in biocrusts versus hypoliths
291 ($P < 0.01$). The Type I and Type II Secretions Systems (T1SS and T2SS, respectively) were also
292 significantly more abundant in biocrusts (Figure 5). These, along with T2SS-associated Sec
293 system, transport a large variety of protein substrates into the extracellular environment. Finally,
294 Type IV (T4SS), which is most commonly involved in conjugation, was also enriched in
295 biocrusts.

296

297 **Genes and pathways enriched in hypolith versus biocrust communities**

298 Five of the twelve pathways significantly more abundant in hypolith versus biocrust
299 communities were related to the synthesis of antibiotics and secondary metabolites (vancomycin
300 group antibiotics, ansamycin antibiotics, macrolides, polyketide backbones, and polyketide sugar
301 units, Table 2). The biosynthesis of vancomycin group antibiotics is a complex process that
302 requires the synthesis of nonstandard amino acids, assembly of both standard and nonstandard
303 amino acids into a heptapeptide backbone through nonribosomal protein synthesis, chlorination,
304 oxidative cross-linking, synthesis of sugar moieties, and attachment of sugars to the backbone.
305 Six of the eight nonstandard amino acid synthesis genes in the KEGG pathway were enriched in
306 hypolithic communities ($P < 0.01$), as were all three of the required genes for nonribosomal
307 protein synthesis. Multiple genes for chlorination, sugar moiety biosynthesis, and sugar
308 attachment were also significant (Figure 7, Supplemental Table 12).

309 Like vancomycin group antibiotics, ansamycin (including the antibiotic rifamycin)
310 biosynthesis follows a long multi-step pathway. However, ansamycins differ in that the carbon
311 framework is formed by a polyketide backbone. We found that multiple pathways for the

312 synthesis of polyketides were significantly enriched in hypoliths compared to biocrusts (P<0.05,
313 Table 2). Within the KEGG ansamycin biosynthesis pathway, five genes encoding polyketide
314 synthases (which assemble smaller subunits into the larger polyketide backbone) were
315 significantly more abundant in hypoliths versus biocrusts (P<0.01, Supplemental Table). Other
316 significant genes in the pathway encode proteins for modifying the polyketide backbone,
317 synthesizing precursors, and post-synthesis modification (Supplemental Table 13).

318 The methane metabolism pathway was significantly enriched in hypolithic communities
319 versus biocrust communities (P<0.001), which was primarily driven by methanotrophy and
320 methylotrophy genes (Figure 8, Supplemental Table 14). All three subunits of particulate
321 methane monooxygenase (*pmoABC*), which encodes the key enzyme required for aerobic
322 oxidation of methane, were significant (P<0.01) but substantially less abundant than other
323 significant genes within the pathway suggesting that methylotrophy is more common than
324 methanotrophy in hypolith communities. Other significant genes in the pathway suggest the use
325 of two pathways for converting formaldehyde to formate (the H₄MPT dependent multi-step
326 pathway and direct conversion via glutathione-independent formaldehyde dehydrogenase),
327 which is corroborated by the high abundance of genes related to the synthesis of coenzymes
328 required in the H₄MPT pathways (specifically coenzyme F420). The data also indicate the use of
329 the serine pathway for formaldehyde assimilation.

330

331 **Effects of dominant primary producer (moss versus cyanobacteria) on functional potential**

332 We observed differences in functional potential in moss- versus cyanobacteria-dominated
333 communities independent of the ecological niche (Supplemental Tables 15 & 16), though fewer
334 pathways were significantly different in moss versus cyanobacterial comparisons (14 pathways)

335 than in biocrust versus hypolith comparisons (23 pathways) (Tables 3 & 4). In cyanobacteria-
336 dominated samples, most significantly enriched pathways (four of seven) were related to
337 cyanobacterial metabolism—specifically photosynthesis, antenna proteins, carotenoid
338 biosynthesis, and porphyrin and chlorophyll metabolism. An additional pathway, ubiquinone,
339 and other terpenoid-quinone biosynthesis, was significant in cyanobacterial-dominated
340 communities due to the high abundance of vitamin E (produced exclusively by photosynthetic
341 organisms) synthesis genes.

342 In moss-dominated samples, the ATP-binding cassette (ABC) transporters pathway was
343 significantly more abundant than in cyanobacterial communities. The ABC transport system
344 couples ATP hydrolysis with the transport of substrates across the membrane. Transporters
345 typically consist of multiple components, including transmembrane domains, ATP-hydrolyzing
346 domains, and a substrate-binding protein. A total of 66 genes within the pathway were significant
347 ($P < 0.01$, Figure 9, Supplemental Table 17) and primarily encode monosaccharide and amino
348 acid transporters. Genes related to the uptake of osmoprotectants (e.g., glycine betaine, proline,
349 putrescine) and precursors for the synthesis of stress related molecules (arginine/ornithine) were
350 also significant.

351

352 **Discussion**

353 Our investigations revealed that the functional repertoire of surface communities in dryland
354 ecosystems is strongly shaped by ecological niche (biocrust versus hypolith) and, to a lesser
355 degree, dominant primary producer (moss versus cyanobacteria). Relative to niche and primary
356 producer, location and season (Sheep Creek Wash collected in March and Granite Mountains
357 Reserve collected in August) had a substantially reduced effect on functional potential. This

358 observation suggests that the functions identified here likely play conserved roles in the ecology
359 of the different environmental niches distributed in dryland soils. As hypothesized, genes and
360 pathways enriched in biocrusts relative to hypoliths reflect adaptation to heat and desiccation
361 stressors. These communities showed an increased capacity for DNA repair, motility,
362 environmental stimuli sensing and response, and interactions with other community members.
363 On the other hand, hypolithic communities were enriched in antibiotic and secondary metabolite
364 synthesis pathways. Moss-dominated samples showed an increased abundance of genes for the
365 uptake of monosaccharides, amino acids, and osmoprotectants relative to cyanobacteria-
366 dominated samples, which may reflect leakage of these substrates by moss gametophyte tissues
367 (the “bryotic pulse”) (21).

368 Given that severe prolonged water deprivation exerts extreme stress on microbial
369 communities, we expected to find differences in samples collected March, where rainfall had
370 occurred within 2-3 days prior to collection, and August, where communities had experienced
371 months of extreme heat without recent precipitation. We also predicted that geographic location
372 might affect community functional potential due to climatic differences between sites. The
373 Wrightwood site experiences cooler annual temperatures and higher precipitation (average high
374 and low annual temperatures 16.8°C and 1.7°C, average annual precipitation 49.4 cm) compared
375 to the Granite Mountains site (annual high and low temperatures 26.5°C and 3.5°C, average
376 annual precipitation 22 cm) (Wrightwood Weather Station, NOAA National Climatic Data
377 Center; Granites Weather Station, UC Natural Reserve System). Instead, collection month and
378 location had minor effects compared to niche and dominant primary producers. This suggests
379 that biocrust and hypolithic communities are resilient to the stressors imposed by environmental
380 extremes and that these taxa have high degrees of physiological flexibility that enable them to

381 maintain consistent abundances during seasonal fluctuations (53–55). This is opposed to a model
382 where taxa adapted to specific seasonal environmental conditions (and their genes) change in
383 abundance with yearly cycles. In the future, the resilience of these communities and their
384 physiological plasticity could be further investigated by tracking concurrent changes in
385 taxonomy, function, and functional potential across seasons. Our data also suggest that factors
386 characteristic of the two niches we investigated are more important than geographic distance and
387 broad climatic similarities in determining functional potential. This observation has played out
388 on an even larger scale, where studies have demonstrated that hypolithic communities in cold
389 and hot desert environments share more similarities with each other than with non-hypolithic
390 soils (8).

391

392 **DNA repair**

393 Desiccation and high UV exposure induce multiple types of DNA damage, which is
394 countered by a variety of repair mechanisms. Hypolithic communities colonize the ventral sides
395 of semi-translucent stones, which filter UV radiation and increase moisture availability.
396 Hypolithic communities also experience an attenuation of daily high and low temperature
397 extremes (36), whereas biocrust communities must persist without this protective buffer. Our
398 data show that biocrust communities have an increased capacity for DNA damage repair, likely
399 to counteract the effects of UV and desiccation. We speculate that enrichment of DNA repair
400 genes may be due to increased copy numbers in biocrust genomes. Previous work from Negev
401 Desert biocrusts demonstrated that taxa highly specialized for the desert crust environment
402 contained multiple copies of double-stranded break repair genes in their genomes (35), which
403 may enhance expression or produce proteins with alternative activities or specificities. An

404 analogous scenario holds for the genome of the common biocrust moss, *S. caninervis*, which
405 contains a highly expanded repertoire of protective *ELIP* genes (37), a signature of physiological
406 desiccation and UV tolerance in land plants (56). The higher abundance of DNA repair genes
407 may also be because biocrust taxa on average possess more repair mechanisms and pathways
408 than hypolith taxa. Previous studies have shown uneven distributions of DNA repair pathways
409 across taxa, and suggest the number of repair systems may be related to desiccation and UV
410 tolerance (57). Future work should enable further investigations into these explanations through
411 genomes assembled from metagenomic sequence data.

412

413 **Intercellular competition and antibiotic synthesis**

414 The differential abundance of bacterial secretion systems, quorum sensing genes, biofilm
415 formation genes, and antibiotic synthesis pathways suggests intercellular interactions play an
416 important role in niche specialization in dryland communities. Competition for finite resources
417 through eliminating competitors appears to be crucial in both biocrust and hypolith communities
418 (58), but the strategies for doing so have diverged. Biocrusts have a greater capacity to use the
419 T6SS as a weapon of interbacterial competition, whereas hypoliths have an increased ability to
420 produce multiple classes of antibiotics. T6SSs deliver toxic effector proteins to the cytoplasm of
421 target cells through a tubular device that extends to puncture the cell envelope (59). Such
422 interactions require direct cell-to-cell contact, suggesting higher encounter rates between cells.
423 This is consistent with previous observations that T6SS-bearing cells are more abundant in
424 environments with closer cell proximities (60). Conversely, the production of antibiotics may
425 reflect a more open system and higher moisture content, enabling metabolites to diffuse away
426 from cells. The greater abundance of biofilm-related genes in biocrusts than hypoliths is

427 consistent with increased opportunities for direct cellular interactions. Cells are packed densely
428 in biofilms (61), which may facilitate the direct contact necessary for the T6SS to deliver toxins
429 to neighboring cells. In hypoliths, increased moisture availability via condensation and slower
430 rates of evaporation (36) may facilitate the diffusion of compounds between cells, favoring the
431 use of antibiotics. To a lesser degree, we also observed a significant enrichment of antibiotic
432 synthesis pathways in samples containing moss as the primary producer. The association of
433 antibiotic synthesis with the presence of moss might also reflect the increased availability of
434 moisture to enable diffusion of antibiotics, as mosses possess morphological features (e.g., leaf
435 and branch architecture, leaf papillae, and leaf hair points) that are specialized for the
436 sequestration, transport, and retention of external water (62, 63). We note that the enrichment of
437 antibiotic synthesis pathways in hypoliths compared with biocrusts does not imply biocrusts lack
438 this ability. Indeed, biocrusts may contain more of these genes and pathways than other soil
439 types. Biocrusts were previously found to harbor a diversity of biosynthetic gene clusters, which
440 were crucial for niche differentiation and maintenance (64).

441 Canonically, bacterial antibiotic production has been viewed as a weapon in competitive
442 battles (65), but alternative hypotheses suggest that sub-inhibitory concentrations may play a role
443 in intercellular signaling (66, 67). Recent studies designed to distinguish between the hypotheses
444 strongly indicate that antibiotics act as weapons of interbacterial competition (68, 69).

445 Regardless, the diversity and abundance of antibiotic synthesis genes suggest this environment is
446 a large potential untapped resource that could aid in addressing the mounting public health crisis
447 of widespread antibiotic resistance in pathogens. Bacterial soil isolates represent a major source
448 of modern antibiotics and other metabolites useful in medicine and biotechnology. However, the
449 use of environmental bacteria for antibiotic discovery has slowed due to high rates of antibiotic

450 rediscovery and because only a small fraction of isolates produce useful metabolites (70, 71).
451 Here, deep sequencing of the uncultured majority provides a resource that could be used to
452 overcome this hurdle either through targeted cultivation or synthetic biology, potentially
453 revealing novel compounds useful in the clinic and beyond (70, 72).

454

455 **Environmental sensing and response via the two-component regulatory system**

456 Two component systems are found in nearly all bacterial genomes, but those that inhabit
457 rapidly changing or diverse environments typically encode a large number of two component
458 system genes, suggesting that organisms expand their repertoire to adapt to environmental
459 challenges (48, 73). The high prevalence in biocrust communities, which are exposed to more
460 extremes than hypolith communities, is consistent with this observation suggesting that sensing
461 and responding to local conditions and stressors play a key role in adaptation to the biocrust
462 ecological niche. Since the input signal and cellular response of a given system can often be
463 predicted based on DNA sequence, the specific two-component system genes that are enriched in
464 a particular environment can be used to infer which environmental stimuli microbial
465 communities are attuned to and the subsequent downstream response (46). In the case of biocrust
466 communities, these adaptations include motility and chemotaxis, surface adhesion and biofilm
467 formation, redox conditions, nutrient limitation, and environmental stressors, all of which may be
468 particularly important for organisms inhabiting oligotrophic environments with transient pulses
469 of nutrient availability and metabolic activity (55, 74, 75). Biocrusts are poikiloydric
470 communities with the ability to desiccate completely during extended dry periods and quickly
471 resume metabolic activity when moisture becomes available (1). Heterotrophic organisms in
472 these communities must thus maintain the capacity to respond quickly to changes in their

473 environment and exploit resources generated by primary producers during brief pulses of
474 hydration and metabolic activity. Moss-dominated biocrusts produce vertical strata, with
475 gradients of light, moisture, UV exposure, and nutrients lost from moss leaf cells during
476 rehydration (21). It is likely critical for microorganisms to optimize and maintain their position
477 relative to the spatial distribution of these variables within the moss biocrust. Similarly, the
478 microbial community associated with the common early-successional cyanobacterium
479 *Microcoleus* (the “cyanosphere”, (30)) is also likely to harbor adaptations to chemotaxis and
480 motility, as *Microcoleus* moves vertically within the soil surface in response to moisture
481 availability (76).

482

483 **Methylotrophy, photosynthesis, and CO₂ fixation in hypolithic communities**

484 The enrichment in genes related to methylotrophy in hypoliths compared to biocrust
485 communities could reflect a higher abundance of moss-associated Methylobacteria in hypoliths.
486 Methylobacteria are known to live as epiphytes on plants, including mosses, where they utilize
487 methanol emitted as a byproduct of pectin degradation in cell walls during cell division and
488 growth (77). We note that if the moss-associated methylotrophs were the sole explanation for
489 the high abundance of methylotrophy genes in hypoliths, we should also have observed a
490 corresponding enrichment of the methane metabolism pathway in moss- versus cyanobacteria-
491 dominated samples, which was not apparent at the conservative threshold we used to identify
492 differentially abundant genes ($P < 0.01$). However, when a threshold of $P < 0.05$ was applied,
493 most of the methotrophy genes that were enriched in hypoliths versus biocrusts were also
494 enriched when comparing moss versus cyanobacterial samples. This suggests the enrichment
495 observed in hypoliths may be due to higher abundances of moss-associated methylotrophs in

496 hypolithic microsites plus other yet unknown metabolic processes resulting the availability of C1
497 substrates to methylotrophic communities. In hypolithic communities, we also found that
498 photosynthesis and CO₂ fixation pathways were more abundant than in biocrusts, which might be
499 explained by a higher abundance of cyanobacteria relative to other microbial taxa in hypoliths
500 (10).

501 This study represents an overview of the functional potential of biocrust and hypolith
502 microbial communities. By using reads rather than assembled data, we were able to capture
503 sequences from low abundance taxa and avoid biases introduced by assembling and binning
504 metagenomic sequence data (78), thus providing quantitative information on gene relative
505 abundances. Ongoing work that includes assembly and constructing metagenome assembled
506 genomes will provide complementary information, revealing how functions are partitioned
507 among community members and enabling us to address questions generated by read-based
508 analyses such as whether enhanced DNA repair abilities in biocrust communities are due to copy
509 number variation, more DNA repair pathways, or a combination of the two. We mitigated issues
510 associated with read-based analyses such as mis-annotations due to short read length by using an
511 extremely conservative approach, setting a low p-value threshold ($P > 0.01$) and requiring that
512 many genes within a pathway reach significance.

513

514 **Concluding remarks**

515 In dryland regions where hypoliths and biocrusts are intermingled on the soil surface, both
516 niches share superficial similarities, such as primary producers, which motivated us to question
517 how the microbial communities associated with these proximate yet distinct microsites might

518 differ. We found that niche (biocrust or hypolith) had a stronger influence on functional pathway
519 differences than primary producers (moss or cyanobacteria). The importance of environmental
520 stressors such as desiccation, extreme daily temperature fluctuations, and UV exposure was
521 reflected in the significant enrichment of pathways associated with responding to and mitigating
522 these stresses in biocrusts as opposed to hypoliths. Contrasting strategies for competition that we
523 observed in our comparisons may reflect different conditions promoted by niche and primary
524 producers and highlight hypoliths and moss biocrusts as potential sources of novel antibiotics.
525 Notably, the functional signal generated by niche and primary producers greatly overshadowed
526 the influence of spatial (collection site) or temporal (season) variations, highlighting the
527 deterministic nature of these communities. The consistency of functional pathways across
528 divergent environmental conditions suggests that the communities we sampled may be relatively
529 stable, relying on physiological plasticity and/or intermittent quiescence (dormancy) for survival
530 as opposed to compositional turnover.

531

532 **Acknowledgements:**

533 Metagenomic sequencing for this project was provided by the Department of Energy Joint
534 Genome Institute (JGI) through a Community Science Program award (CSP 504034) to K.
535 Fisher and P. Vaishampayan, and R. Mackelprang. This work was also supported by a National
536 Science Foundation Dimensions of Biodiversity Program award to K. Fisher (DOB 1638996).
537 Jameka Jefferson and Amy Vasquez assisted with the preparation and DNA extraction of
538 samples used for this study. Thank you to Jameka Jefferson and Jenna Ekwealor for field
539 assistance, and the Sweeny Granite Mountains Desert Research Center for facilitating sample
540 collection.

541

542 **Competing Interests**

543 The authors declare no competing interests

544

545 **References**

546 1. Belnap J. 2003. The world at your feet: desert biological soil crusts. *Front Ecol Environ*

547 1:181–189.

548 2. Eldridge DJ, Reed S, Travers SK, Bowker MA, Maestre FT, Ding J, Havrilla C, Rodriguez-

549 Caballero E, Barger N, Weber B, Antoninka A, Belnap J, Chaudhary B, Faist A, Ferrenberg

550 S, Huber-Sannwald E, Malam Issa O, Zhao Y. 2020. The pervasive and multifaceted

551 influence of biocrusts on water in the world’s drylands. *Glob Chang Biol* 26:6003–6014.

552 3. Chamizo S, Rodríguez-Caballero E, Román JR, Cantón Y. 2017. Effects of biocrust on soil

553 erosion and organic carbon losses under natural rainfall. *Catena* 148:117–125.

554 4. Rodriguez-Caballero E, Belnap J, Büdel B, Crutzen PJ, Andreae MO, Pöschl U, Weber B.

555 2018. Dryland photoautotrophic soil surface communities endangered by global change.

556 *Nature Geoscience*.

557 5. Chan Y, Lacap DC, Lau MCY, Ha KY, Warren-Rhodes KA, Cockell CS, Cowan DA,

558 McKay CP, Pointing SB. 2012. Hypolithic microbial communities: between a rock and a

559 hard place. *Environ Microbiol* 14:2272–2282.

- 560 6. Makhalanyane TP, Valverde A, Lacap DC, Pointing SB, Tuffin MI, Cowan DA. 2013.
561 Evidence of species recruitment and development of hot desert hypolithic communities.
562 *Environ Microbiol Rep* 5:219–224.
- 563 7. Stomeo F, Valverde A, Pointing SB, McKay CP, Warren-Rhodes KA, Tuffin MI, Seely M,
564 Cowan DA. 2013. Hypolithic and soil microbial community assembly along an aridity
565 gradient in the Namib Desert. *Extremophiles* 17:329–337.
- 566 8. Le PT, Makhalanyane TP, Guerrero LD, Vikram S, Van de Peer Y, Cowan DA. 2016.
567 Comparative Metagenomic Analysis Reveals Mechanisms for Stress Response in Hypoliths
568 from Extreme Hyperarid Deserts. *Genome Biol Evol* 8:2737–2747.
- 569 9. Vikram S, Guerrero LD, Makhalanyane TP, Le PT, Seely M, Cowan DA. 2016.
570 Metagenomic analysis provides insights into functional capacity in a hyperarid desert soil
571 niche community. *Environ Microbiol* 18:1875–1888.
- 572 10. Fisher K, Jefferson JS, Vaishampayan P. 2020. Bacterial Communities of Mojave Desert
573 Biological Soil Crusts Are Shaped by Dominant Photoautotrophs and the Presence of
574 Hypolithic Niches. *Frontiers in Ecology and Evolution* 7:518.
- 575 11. Antoninka A, Bowker MA, Reed SC, Doherty K. 2016. Production of greenhouse-grown
576 biocrust mosses and associated cyanobacteria to rehabilitate dryland soil function. *Restor*
577 *Ecol* 24:324–335.
- 578 12. Wood AJ, Oliver MJ. 1999. Translational control in plant stress: the formation of messenger
579 ribonucleoprotein particles (mRNPs) in response to desiccation of *Tortula ruralis*
580 gametophytes. *Plant J* 18:359–370.

- 581 13. Oliver MJ, Velten J, Mishler BD. 2005. Desiccation tolerance in bryophytes: a reflection of
582 the primitive strategy for plant survival in dehydrating habitats? *Integr Comp Biol* 45:788–
583 799.
- 584 14. Oliver MJ, Farrant JM, Hilhorst HWM, Mundree S, Williams B, Bewley JD. 2020.
585 Desiccation tolerance: Avoiding cellular damage during drying and rehydration. *Annu Rev*
586 *Plant Biol* 71:435–460.
- 587 15. Baubin C, Ran N, Siebner H, Gillor O. 2021. The response of desert biocrust bacterial
588 communities to hydration-desiccation cycles.
- 589 16. Coe KK, Belnap J, Sparks JP. 2012. Precipitation-driven carbon balance controls
590 survivorship of desert biocrust mosses. *Ecology* 93:1626–1636.
- 591 17. Coe KK, Sparks JP. 2014. Physiology-based prognostic modeling of the influence of
592 changes in precipitation on a keystone dryland plant species. *Oecologia* 176:933–942.
- 593 18. Reed SC, Coe KK, Sparks JP, Housman DC, Zelikova TJ, Belnap J. 2012. Changes to
594 dryland rainfall result in rapid moss mortality and altered soil fertility. *Nat Clim Chang*
595 2:752–755.
- 596 19. Tuba Z, Protor CF, Csintalan Z. 1998. Ecophysiological responses of homoiochlorophyllous
597 and poikilochlorophyllous desiccation tolerant plants: a comparison and an ecological
598 perspective. *Plant Growth Regul* 24:211–217.
- 599 20. Coe KK, Greenwood JL, Slate ML, Clark TA, Brinda JC, Fisher KM, Mishler BD, Bowker
600 MA, Oliver MJ, Ebrahimi S, Stark LR. 2021. Strategies of desiccation tolerance vary across
601 life phases in the moss *Syntrichia caninervis*. *Am J Bot* 108:249–262.

- 602 21. Slate ML, Sullivan BW, Callaway RM. 2019. Desiccation and rehydration of mosses greatly
603 increases resource fluxes that alter soil carbon and nitrogen cycling. *J Ecol* 107:1767–1778.
- 604 22. Maier S, Tamm A, Wu D, Caesar J, Grube M, Weber B. 2018. Photoautotrophic organisms
605 control microbial abundance, diversity, and physiology in different types of biological soil
606 crusts. *ISME J* 12:1032–1046.
- 607 23. Maier S, Schmidt TSB, Zheng L, Peer T, Wagner V, Grube M. 2014. Analyses of dryland
608 biological soil crusts highlight lichens as an important regulator of microbial communities.
609 *Biodivers Conserv* 23:1735–1755.
- 610 24. Delgado-Baquerizo M, Maestre FT, Eldridge DJ, Bowker MA, Ochoa V, Gozalo B,
611 Berdugo M, Val J, Singh BK. 2016. Biocrust-forming mosses mitigate the negative impacts
612 of increasing aridity on ecosystem multifunctionality in drylands. *New Phytol* 209:1540–
613 1552.
- 614 25. Liu L, Liu Y, Hui R, Xie M. 2017. Recovery of microbial community structure of biological
615 soil crusts in successional stages of Shapotou desert revegetation, northwest China. *Soil Biol
616 Biochem* 107:125–128.
- 617 26. Maestre FT, Castillo-Monroy AP, Bowker MA, Ochoa-Hueso R. 2012. Species richness
618 effects on ecosystem multifunctionality depend on evenness, composition and spatial
619 pattern. *J Ecol* 100:317–330.
- 620 27. Delgado-Baquerizo M, Maestre FT, Eldridge DJ, Bowker MA, Jeffries TC, Singh BK. 2018.
621 Biocrust-forming mosses mitigate the impact of aridity on soil microbial communities in
622 drylands: observational evidence from three continents. *New Phytol* 220:824–835.

- 623 28. Belnap J, Wilcox BP, Van Scoyoc MW, Phillips SL. 2013. Successional stage of biological
624 soil crusts: an accurate indicator of ecohydrological condition. *Ecohydrology* 6:474–482.
- 625 29. Weber B, Bowker M, Zhang Y, Belnap J. 2016. Natural recovery of biological soil crusts
626 after disturbance, p. 479–498. *In* *Biological Soil Crusts: An Organizing Principle in*
627 *Drylands*. Springer International Publishing, Cham.
- 628 30. Couradeau E, Giraldo-Silva A, De Martini F, Garcia-Pichel F. 2019. Spatial segregation of
629 the biological soil crust microbiome around its foundational cyanobacterium, *Microcoleus*
630 *vaginatus*, and the formation of a nitrogen-fixing cyanosphere. *Microbiome* 7:55.
- 631 31. Pointing SB. 2016. Hypolithic Communities, p. 199–213. *In* Weber, B, Büdel, B, Belnap, J
632 (eds.), *Biological Soil Crusts: An Organizing Principle in Drylands*. Springer International
633 Publishing, Cham.
- 634 32. Cowan DA, Khan N, Pointing SB, Cary SC. 2010. Diverse hypolithic refuge communities in
635 the McMurdo Dry Valleys. *Antarct Sci* 22:714–720.
- 636 33. de los Ríos A, Cary C, Cowan D. 2014. The spatial structures of hypolithic communities in
637 the Dry Valleys of East Antarctica. *Polar Biol* 37:1823–1833.
- 638 34. Cowan DA, Sohm JA, Makhalanyane TP, Capone DG, Green TGA, Cary SC, Tuffin IM.
639 2011. Hypolithic communities: important nitrogen sources in Antarctic desert soils. *Environ*
640 *Microbiol Rep* 3:581–586.
- 641 35. Meier DV, Imminger S, Gillor O, Woebken D. 2021. Distribution of Mixotrophy and
642 Desiccation Survival Mechanisms across Microbial Genomes in an Arid Biological Soil
643 Crust Community. *mSystems* 6.

- 644 36. Ekwealor JTB, Fisher KM. 2020. Life under quartz: Hypolithic mosses in the Mojave
645 Desert. PLoS One 15:e0235928.
- 646 37. Silva AT, Gao B, Fisher KM, Mishler BD, Ekwealor JTB, Stark LR, Li X, Zhang D,
647 Bowker MA, Brinda JC, Coe KK, Oliver MJ. 2021. To dry perchance to live: Insights from
648 the genome of the desiccation-tolerant biocrust moss *Syntrichia caninervis*. Plant J
649 105:1339–1356.
- 650 38. Bushnell B. BBTools.
- 651 39. Kanehisa M, Goto S, Sato Y, Kawashima M, Furumichi M, Tanabe M. 2014. Data,
652 information, knowledge and principle: back to metabolism in KEGG. Nucleic Acids Res
653 42:D199-205.
- 654 40. Buchfink B, Xie C, Huson DH. 2015. Fast and sensitive protein alignment using
655 DIAMOND. Nat Methods 12:59–60.
- 656 41. McMurdie PJ, Holmes S. 2013. phyloseq: an R package for reproducible interactive analysis
657 and graphics of microbiome census data. PLoS One 8:e61217.
- 658 42. R Core Team. 2021. R: A Language and Environment for Statistical Computing. R
659 Foundation for Statistical Computing, Vienna, Austria.
- 660 43. Oksanen J, Kindt R, Legendre P, O’Hara B, Stevens MHH, Oksanen MJ, Suggests M. 2007.
661 The vegan package. Community ecology package 10:719.

- 662 44. McCarthy DJ, Chen Y, Smyth GK. 2012. Differential expression analysis of multifactor
663 RNA-Seq experiments with respect to biological variation. *Nucleic Acids Res* 40:4288–
664 4297.
- 665 45. Kolde R. 2019. pheatmap: Pretty Heatmaps.
- 666 46. Mackelprang R, Burkert A, Haw M, Mahendrarajah T, Conaway CH, Douglas TA, Waldrop
667 MP. 2017. Microbial survival strategies in ancient permafrost: insights from metagenomics.
668 *ISME J* 11:2305–2318.
- 669 47. Benjamini Y, Hochberg Y. 1995. Controlling the false discovery rate: A practical and
670 powerful approach to multiple testing. *J R Stat Soc* 57:289–300.
- 671 48. Capra EJ, Laub MT. 2012. Evolution of two-component signal transduction systems. *Annu*
672 *Rev Microbiol* 66:325–347.
- 673 49. Francez-Charlot A, Kaczmarczyk A, Vorholt JA. 2015. The branched CcsA/CckA-ChpT-
674 CtrA phosphorelay of *Sphingomonas melonis* controls motility and biofilm formation. *Mol*
675 *Microbiol* 97:47–63.
- 676 50. Zan J, Heindl JE, Liu Y, Fuqua C, Hill RT. 2013. The CckA-ChpT-CtrA phosphorelay
677 system is regulated by quorum sensing and controls flagellar motility in the marine sponge
678 symbiont *Ruegeria* sp. KLH11. *PLoS One* 8:e66346.
- 679 51. Elsen S, Swem LR, Swem DL, Bauer CE. 2004. RegB/RegA, a highly conserved redox-
680 responding global two-component regulatory system. *Microbiol Mol Biol Rev* 68:263–279.

- 681 52. Danson AE, Jovanovic M, Buck M, Zhang X. 2019. Mechanisms of σ^{54} -Dependent
682 Transcription Initiation and Regulation. *J Mol Biol* 431:3960–3974.
- 683 53. Allison SD, Martiny JBH. 2008. Resistance, resilience, and redundancy in microbial
684 communities. *Proceedings of the National Academy of Sciences*.
- 685 54. Green TGA, Proctor MCF. 2016. Physiology of Photosynthetic Organisms Within
686 Biological Soil Crusts: Their Adaptation, Flexibility, and Plasticity, p. 347–381. *In* Weber,
687 B, Büdel, B, Belnap, J (eds.), *Biological Soil Crusts: An Organizing Principle in Drylands*.
688 Springer International Publishing, Cham.
- 689 55. Rajeev L, da Rocha UN, Klitgord N, Luning EG, Fortney J, Axen SD, Shih PM, Bouskill
690 NJ, Bowen BP, Kerfeld CA, Garcia-Pichel F, Brodie EL, Northen TR, Mukhopadhyay A.
691 2013. Dynamic cyanobacterial response to hydration and dehydration in a desert biological
692 soil crust. *ISME J* 7:2178–2191.
- 693 56. VanBuren R, Pardo J, Man Wai C, Evans S, Bartels D. 2019. Massive Tandem Proliferation
694 of ELIPs Supports Convergent Evolution of Desiccation Tolerance across Land Plants. *Plant*
695 *Physiol* 179:1040–1049.
- 696 57. Cassier-Chauvat C, Veaudor T, Chauvat F. 2016. Comparative Genomics of DNA
697 Recombination and Repair in Cyanobacteria: Biotechnological Implications. *Front*
698 *Microbiol* 7:1809.
- 699 58. Ghoul M, Mitri S. 2016. The Ecology and Evolution of Microbial Competition. *Trends*
700 *Microbiol* 24:833–845.

- 701 59. Durand E, Nguyen VS, Zoued A, Logger L, Péhau-Arnaudet G, Aschtgen M-S, Spinelli S,
702 Desmyter A, Bardiaux B, Dujeancourt A, Roussel A, Cambillau C, Cascales E, Fronzes R.
703 2015. Biogenesis and structure of a type VI secretion membrane core complex. *Nature*
704 523:555–560.
- 705 60. Kempnich MW, Sison-Mangus MP. 2020. Presence and abundance of bacteria with the
706 Type VI secretion system in a coastal environment and in the global oceans. *PLoS One*
707 15:e0244217.
- 708 61. Xavier JB, Foster KR. 2007. Cooperation and conflict in microbial biofilms. *Proc Natl Acad*
709 *Sci U S A* 104:876–881.
- 710 62. Giordano S, Colacino C, Spagnuolo V, Basile A, Esposito A, Castaldo-Cobianchi R. 1993.
711 Morphological adaptation to water uptake and transport in the poikilohydric moss *Tortula*
712 *ruralis*. *G Bot Ital* 127:1123–1132.
- 713 63. Pan Z, Pitt WG, Zhang Y, Wu N, Tao Y, Truscott TT. 2016. The upside-down water
714 collection system of *Syntrichia caninervis*. *Nat Plants* 2:16076.
- 715 64. Van Goethem MW, Osborn AR, Bowen BP, Andeer PF, Swenson TL, Clum A, Riley R, He
716 G, Koriabine M, Sandor L, Yan M, Daum CG, Yoshinaga Y, Makhalanyane TP, Garcia-
717 Pichel F, Visel A, Pennacchio LA, O'Malley RC, Northen TR. 2021. Long-read
718 metagenomics of soil communities reveals phylum-specific secondary metabolite dynamics.
719 *Communications Biology* 4:1302.
- 720 65. Ratcliff WC, Denison RF. 2011. Microbiology. Alternative actions for antibiotics. *Science*
721 332:547–548.

- 722 66. Romero D, Traxler MF, López D, Kolter R. 2011. Antibiotics as signal molecules. *Chem*
723 *Rev* 111:5492–5505.
- 724 67. Linares JF, Gustafsson I, Baquero F, Martinez JL. 2006. Antibiotics as intermicrobial
725 signaling agents instead of weapons. *Proc Natl Acad Sci U S A* 103:19484–19489.
- 726 68. Abrudan MI, Smakman F, Grimbergen AJ, Westhoff S, Miller EL, van Wezel GP, Rozen
727 DE. 2015. Socially mediated induction and suppression of antibiosis during bacterial
728 coexistence. *Proc Natl Acad Sci U S A* 112:11054–11059.
- 729 69. Westhoff S, van Leeuwe TM, Qachach O, Zhang Z, van Wezel GP, Rozen DE. 2017. The
730 evolution of no-cost resistance at sub-MIC concentrations of streptomycin in *Streptomyces*
731 *coelicolor*. *ISME J* 11:1168–1178.
- 732 70. Hover BM, Kim S-H, Katz M, Charlop-Powers Z, Owen JG, Ternei MA, Maniko J, Estrela
733 AB, Molina H, Park S, Perlin DS, Brady SF. 2018. Culture-independent discovery of the
734 malacidins as calcium-dependent antibiotics with activity against multidrug-resistant Gram-
735 positive pathogens. *Nat Microbiol* 3:415–422.
- 736 71. Reddy BVB, Kallifidas D, Kim JH, Charlop-Powers Z, Feng Z, Brady SF. 2012. Natural
737 product biosynthetic gene diversity in geographically distinct soil microbiomes. *Appl*
738 *Environ Microbiol* 78:3744–3752.
- 739 72. Crits-Christoph A, Diamond S, Butterfield CN, Thomas BC, Banfield JF. 2018. Novel soil
740 bacteria possess diverse genes for secondary metabolite biosynthesis. *Nature* 558:440–444.
- 741 73. Galperin MY. 2005. A census of membrane-bound and intracellular signal transduction
742 proteins in bacteria: bacterial IQ, extroverts and introverts. *BMC Microbiol* 5:35.

- 743 74. Bowker MA, Belnap J, Davidson DW, Phillips SL. 2005. Evidence for Micronutrient
744 Limitation of Biological Soil Crusts: Importance to Arid-Lands Restoration. *Ecol Appl*
745 15:1941–1951.
- 746 75. Swenson TL, Couradeau E, Bowen BP, De Philippis R, Rossi F, Mugnai G, Northen TR.
747 2018. A novel method to evaluate nutrient retention by biological soil crust exopolymeric
748 matrix. *Plant Soil* 429:53–64.
- 749 76. Garcia-Pichel F, Pringault O. 2001. Microbiology. Cyanobacteria track water in desert soils.
750 *Nature* 413:380–381.
- 751 77. Schauer S, Kutschera U. 2011. A novel growth-promoting microbe, *Methylobacterium*
752 *funariae* sp. nov., isolated from the leaf surface of a common moss. *Plant Signal Behav*
753 6:510–515.
- 754 78. Nelson WC, Tully BJ, Mobberley JM. 2020. Biases in genome reconstruction from
755 metagenomic data. *PeerJ* 8:e10119.

756

757

758

759

760

761

762

763

764

765

766

767

768

769

770

771 **Figure legends**

772

773 **Figure 1.** Examples of biocrust and hypolith environments with moss or cyanobacteria as the dominant
774 photoautotroph anchor.

775 **Figure 2. Principle Coordinate Analysis (PCoA) ordination plots of (A) all samples, (B) biocrust**
776 **samples, and (C) hypolith samples.** In panel A, samples are colored according to environmental niche
777 (blue: biocrust, red: hypolith, yellow: bare soil) and shaped by dominant primary producer (circle:
778 cyanobacteria, triangle: moss). Panel B shows biocrust samples, which are colored by primary producer
779 (blue: cyanobacteria, red: moss). Panel C shows hypolith samples, which colored by the same scheme as
780 in panel B.

781 **Figure 3. Heatmap of DNA repair genes significantly more abundant in biocrust communities**
782 **versus hypolith communities.** Genes are shown in rows and samples are shown in columns. Heat map
783 colors show the relative abundances of genes scaled by row. Rows are labeled by gene names. Sample
784 names are colored according to the dominant primary producer and environment. Hypolith samples are
785 indicated by cool colors and biocrust samples are shown by warm colors (light blue: moss hypolith, dark
786 blue: cyanobacterial hypolith, orange: moss biocrust, red: cyanobacterial biocrust). Columns and rows
787 were clustered for visualization purposes using the complete linkage method. DNA repair related
788 functions are indicated by superscripts after the gene names as follows. 1: DNA polymerase III, 2:
789 nucleotide excision repair, 3: replication restart, 4: homologous recombination-based repair, 5: mismatch
790 recognition, 6: endonuclease, 7: base excision repair. A list of genes with the corresponding KEGG
791 orthology numbers can be found in Supplemental Table 6.

792

793

794 **Figure 4. Selected two component systems enriched in biocrust crust communities.** Two component
795 systems canonically contain a sensor kinase (shown as rectangles within the membrane) and response
796 regulator (shown as squares), which mediate downstream cellular responses when phosphorylated.
797 Additional components specific to a particular system are shown in ovals. Phosphate (P) is indicated by
798 yellow circles. Each protein is labeled by the name of the gene that encodes it. Blue indicates genes
799 significantly more abundant in biocrust compared to hypolith communities ($P < 0.01$). Grey shows genes
800 with p-values > 0.01 . Panel A contains lifestyle-related two component systems, B contains two
801 component systems related to redox signals and catabolites, and C contains systems related to nutrient
802 limitation and environmental stressors. This figure highlights systems with strong evidence (i.e., multiple
803 significant genes within the system) of being more abundant in biocrusts versus hypoliths. A complete list
804 of genes within the KEGG two component system pathway that were significant is provided in
805 Supplemental Table 7.

806 **Figure 5. Diagram of the KEGG flagellar assembly pathway.** Genes significantly more abundant in
807 biocrusts versus hypoliths ($P < 0.01$) are indicated in bold text. Genes where $P > 0.01$ are not bolded.
808 KEGG orthology numbers corresponding to gene names are listed in Supplemental Table 8.

809 **Figure 6. Schematic of bacterial secretion systems significantly more abundant in biocrust**
810 **compared with hypolith communities.** Each component is labeled with a gene name. Names in bold
811 represent significant genes ($P < 0.01$) and names in gray represent non-significant genes ($P > 0.01$). A full
812 list of bacterial secretion system genes significantly more abundant in biocrusts versus hypoliths can be
813 found in Supplemental Table 11. The pathway schematic is based on the KEGG secretion system
814 diagram, Costa et al. (2015), and (Mackelprang et al. 2017).

815

816

817 **Figure 7: Overview of vancomycin biosynthesis pathway labeled with genes significantly more**
818 **abundant in hypolith compared with biocrust microbial communities.** Schematic represents all major
819 steps in the pathway, including synthesis of nonproteinogenic amino acids 4-Hydroxyphenylglycine (Hpg)
820 and 3,5-Dihydroxyphenylglycine (Dpg), sugar biosynthesis, assembly of the peptide backbone via
821 nonribosomal proteins synthesis, crosslinking and modification, and sugar attachment. Genes
822 significantly more abundant in hypoliths ($P < 0.01$) are indicated by bold text. KEGG orthology numbers
823 corresponding to genes names are in Supplemental Table 12.

824 **Figure 8. Overview of methanotrophy/methylotrophy pathways enriched in hypolith compared to**
825 **biocrust communities.** Significant genes ($P < 0.01$) are indicated on the diagram. Genes with a p-value $>$
826 0.01 were omitted from the figure. Abbreviations are as follows. OAA: oxaloacetate, PEP:
827 phosphoenolpyruvate, EPPG: enolpyruvoyl-2-diphospho-5'-guanosine. A list of genes and the
828 corresponding KEGG orthology numbers can be found in Supplemental Table 14.

829 **Figure 9: Selected ABC transporters significantly more abundant in moss-dominated samples**
830 **compared to cyanobacteria-dominated samples.** Each system is labeled by the substrate transported.
831 Each component is labeled with the gene name. Colored proteins are significant ($P < 0.01$). Greyed
832 proteins represent genes with a p-value $>$ than 0.01. A complete list of ABC transporter genes that are
833 significantly more abundant in moss-dominated samples are found in Supplemental Table 17.

834

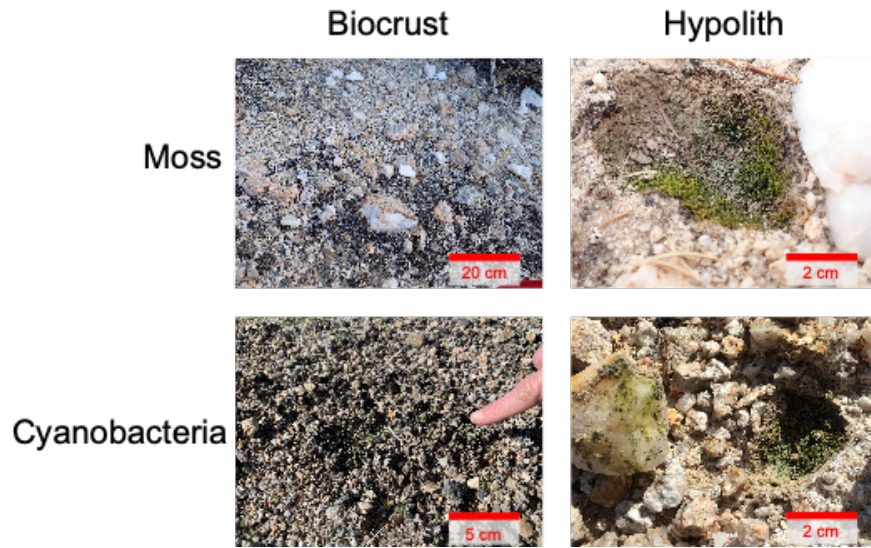


Figure 1. Examples of biocrust and hypolith environments with moss or cyanobacteria as the dominant photoautotroph anchor.

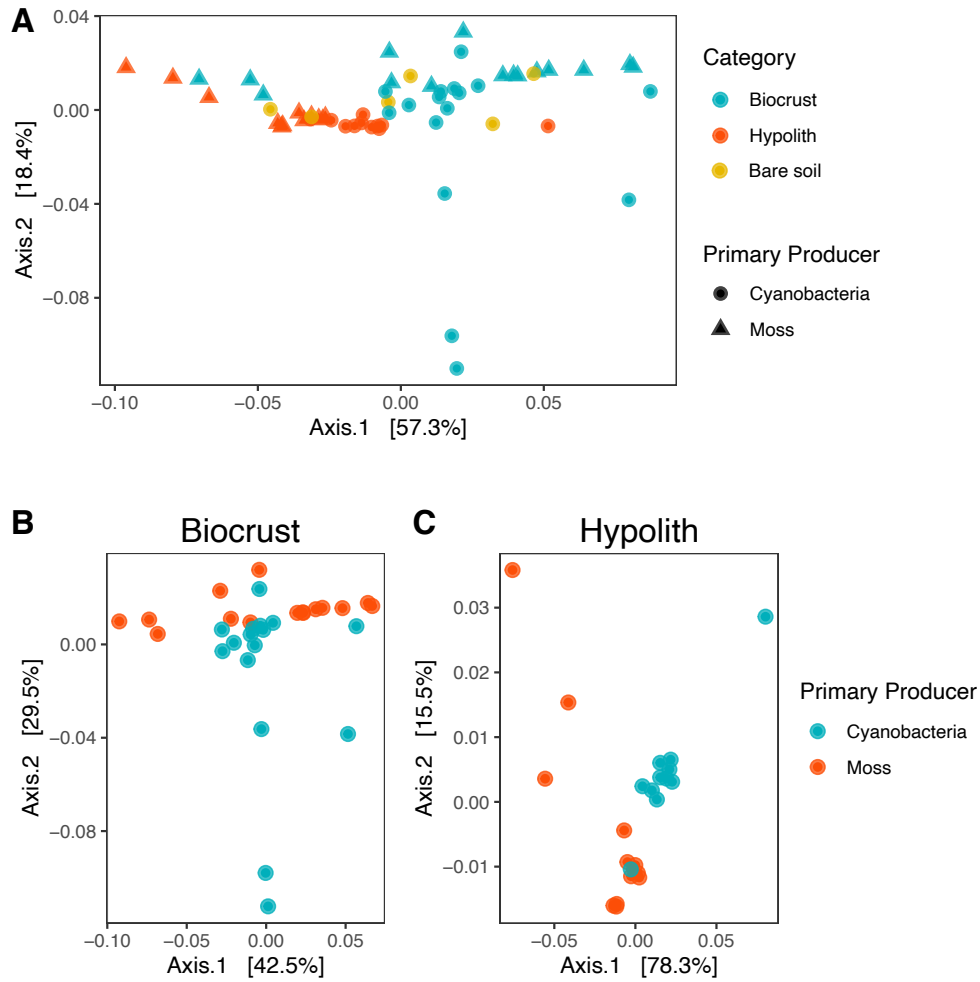


Figure 2. Principle Coordinate Analysis (PCoA) ordination plots of (A) all samples, (B) biocrust samples, and (C) hypolith samples. In panel A, samples are colored according to environmental niche (blue: biocrust, red: hypolith, yellow: bare soil) and shaped by dominant primary producer (circle: cyanobacteria, triangle: moss). Panel B shows biocrust samples, which are colored by primary producer (blue: cyanobacteria, red: moss). Panel C shows hypolith samples, which colored by the same scheme as in panel B.

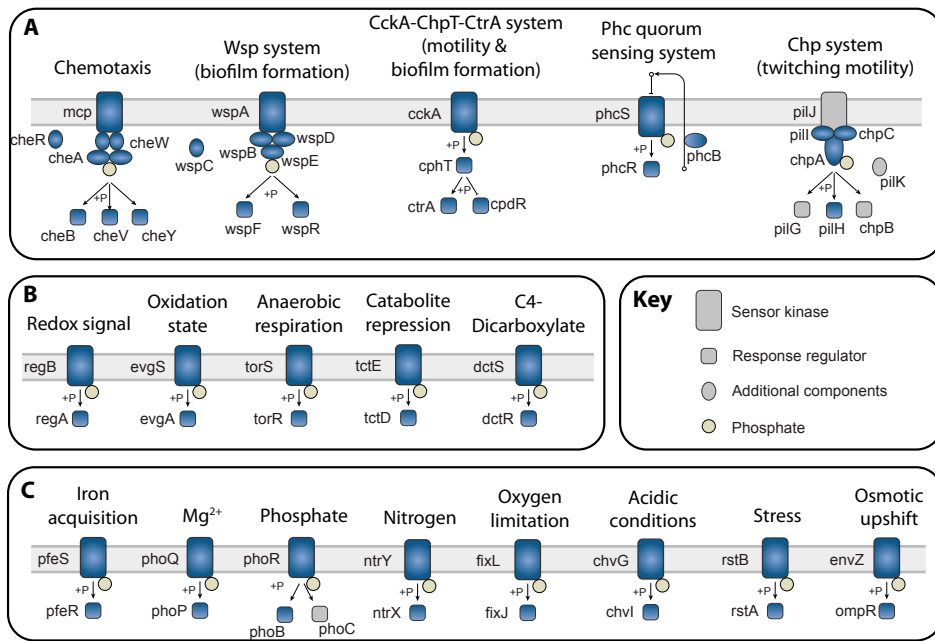


Figure 4. Selected two component systems enriched in biocrust crust communities. Two component systems canonically contain a sensor kinase (shown as rectangles within the membrane) and response regulator (shown as squares), which mediate downstream cellular responses when phosphorylated. Additional components specific to a particular system are shown in ovals. Phosphate (P) is indicated by yellow circles. Each protein is labeled by the name of the gene that encodes it. Blue indicates genes significantly more abundant in biocrust compared to hypolith communities ($P < 0.01$). Grey shows genes with p -values > 0.01 . Panel A contains lifestyle-related two component systems, B contains two component systems related to redox signals and catabolites, and C contains systems related to nutrient limitation and environmental stressors. This figure highlights systems with strong evidence (i.e., multiple significant genes within the system) of being more abundant in biocrusts versus hypoliths. A complete list of genes within the KEGG two component system pathway that were significant is provided in Supplemental Table 7.

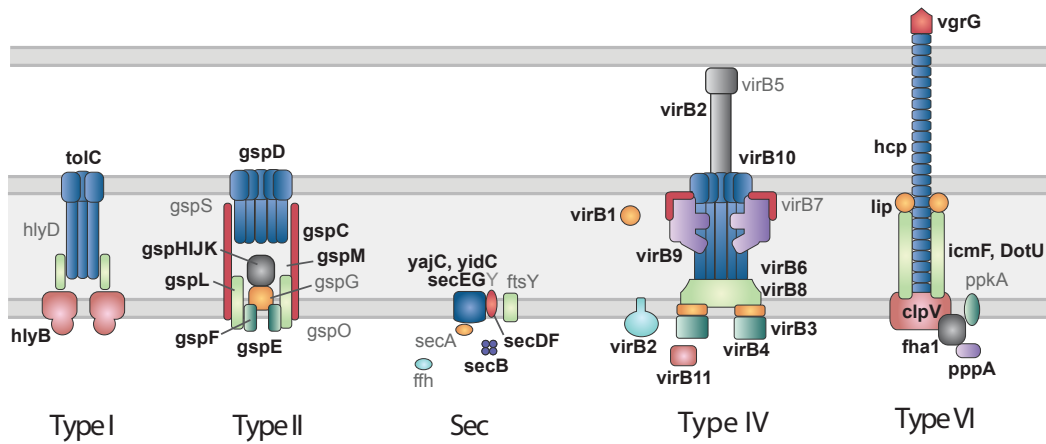


Figure 6. Schematic of bacterial secretion systems significantly more abundant in biocrust compared with hypolith communities. Each component is labeled with a gene name. Names in bold represent significant genes ($P < 0.01$) and names in gray represent non-significant genes ($P > 0.01$). A full list of bacterial secretion system genes significantly more abundant in biocrusts versus hypoliths can be found in Supplemental Table 11. The pathway schematic is based on the KEGG secretion system diagram, Costa et al. (2015), and (Mackelprang et al. 2017).

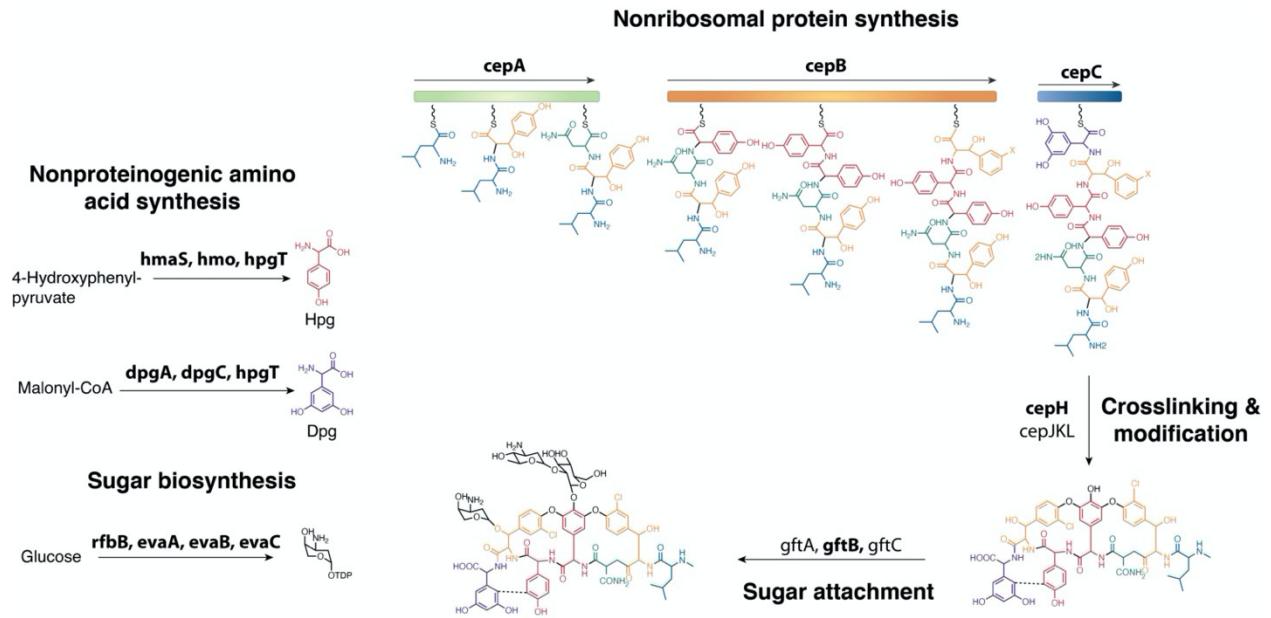
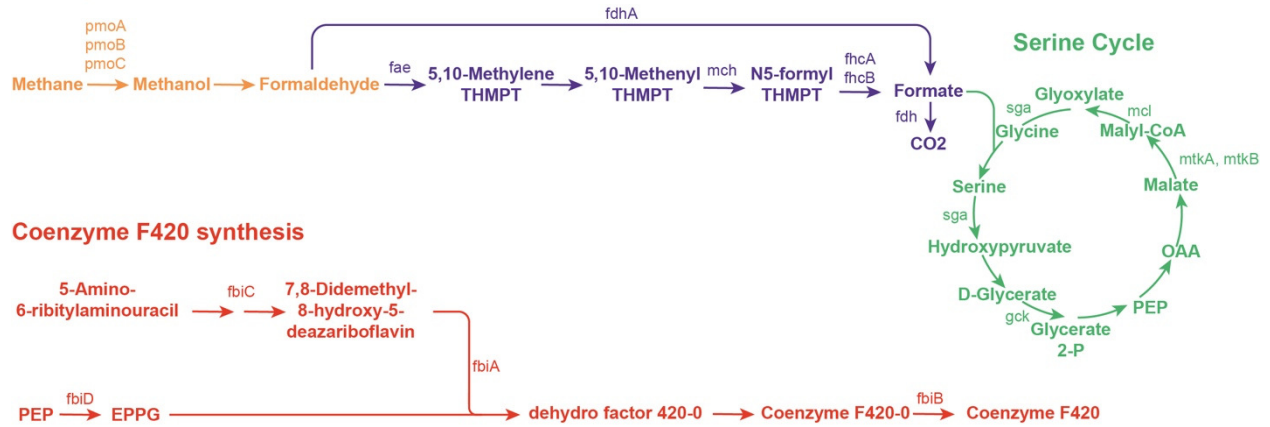


Figure 7: Overview of vancomycin biosynthesis pathway labeled with genes significantly more abundant in hypolith compared with biocrust microbial communities. Schematic represents all major steps in the pathway, including synthesis of nonproteinogenic amino acids 4-Hydroxyphenylglycine (Hpg) and 3,5-Dihydroxyphenylglycine (Dpg), sugar biosynthesis, assembly of the peptide backbone via nonribosomal proteins synthesis, crosslinking and modification, and sugar attachment. Genes significantly more abundant in hypoliths ($P < 0.01$) are indicated by bold text. KEGG orthology numbers corresponding to genes names are in Supplemental Table 12.

Primary Oxidation

Formaldehyde oxidation



74

75

76 **Figure 8. Overview of methanotrophy/methylotrophy pathways enriched in hypolith**

77 **compared to biocrust communities.** Significant genes ($P < 0.01$) are indicated on the diagram.

78 Genes with a p-value > 0.01 were omitted from the figure. Abbreviations are as follows. OAA:

79 oxaloacetate, PEP: phosphoenolpyruvate, EPPG: enolpyruvoyl-2-diphospho-5'-guanosine. A list

80 of genes and the corresponding KEGG orthology numbers can be found in Supplemental Table

81 14.

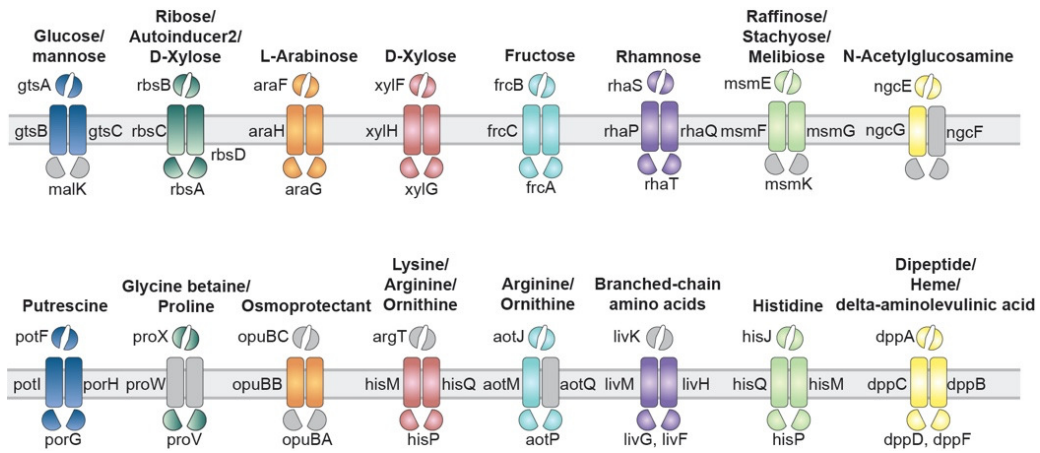
82

83

84

85

86



87

88

89 **Figure 9: Selected ABC transporters significantly more abundant in moss-dominated**

90 **samples compared to cyanobacteria-dominated samples.** Each system is labeled by the

91 substrate transported. Each component is labeled with the gene name. Colored proteins are

92 significant ($P < 0.01$). Greyed proteins represent genes with a p-value $>$ than 0.01. A complete list

93 of ABC transporter genes that are significantly more abundant in moss-dominated samples are

94 found in Supplemental Table 17.

95

Tables

Table 1. KEGG pathways significantly enriched in biocrust versus hypolith communities

Pathway number	Pathway name
ko02020	Two-component system***
ko00540	Flagellar assembly***
ko02040	Cell cycle – Caulobacter***
ko04112	Bacterial secretion system***
ko03070	Bacterial chemotaxis***
ko02030	Lipopolysaccharide biosynthesis***
ko00480	Glutathione metabolism***
ko05111	Biofilm formation - Vibrio cholerae**
ko00550	Peptidoglycan biosynthesis**
ko03060	Protein export**
ko03440	Homologous recombination*

*** P < 0.001

**P < 0.01

*P < 0.05

Table 2. KEGG pathways significantly enriched in hypolith versus biocrust communities

Pathway number	Pathway name
ko01055	Biosynthesis of vancomycin group antibiotics***
ko01051	Biosynthesis of ansamycins***
ko00522	Biosynthesis of 12-, 14- and 16-membered macrolides***
ko01056	Biosynthesis of type II polyketide backbone***
ko03013	RNA transport***
ko00650	Butanoate metabolism***
ko00260	Glycine, serine, and threonine metabolism***
ko00680	Methane metabolism***
Ko00720	Carbon fixation pathways in prokaryotes**
ko00195	Photosynthesis**
ko00523	Polyketide sugar unit biosynthesis*
ko00630	Glyoxylate and dicarboxylate metabolism*

*** P < 0.001

**P < 0.01

*P < 0.05

Table 3. KEGG pathways significantly enriched cyanobacteria-anchored versus moss-anchored communities

Pathway number	Pathway name
ko00195	Photosynthesis***
ko00196	Photosynthesis—antenna proteins***
ko04080	Glutathione metabolism***
ko00906	Carotenoid biosynthesis**
ko00860	Porphyrin and chlorophyll metabolism*
ko00130	Ubiquinone and other terpenoid-quinone biosynthesis*
ko03018	RNA degradation*

*** P < 0.001

**P < 0.01

*P < 0.05

Table 4. KEGG pathways significantly enriched moss-anchored versus cyanobacteria-anchored communities

Pathway number	Pathway name
ko02010	ABC Transporters***
ko01051	Biosynthesis of ansamycins***
ko00524	Neomycin, kanamycin, and gentamicin biosynthesis***
ko00630	Glyoxylate and dicarboxylate metabolism**
ko00650	Butanoate metabolism*
ko00450	Selenocompound metabolism *
ko00362	Benzoate degradation*

*** P < 0.001

**P < 0.01

*P < 0.05